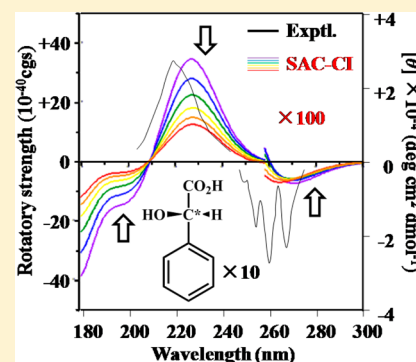


Conformational Dependence of the Circular Dichroism Spectrum of α -Hydroxyphenylacetic Acid: A ChiraSac Study

Tomoo Miyahara*[‡] and Hiroshi Nakatsuji*[‡][‡]Quantum Chemistry Research Institute, JST, CREST, Kyodai Katsura Venture Plaza, North Building 107, 1-36 Goryo-Oohara, Nishikyo-ku, Kyoto 615-8245, Japan

S Supporting Information

ABSTRACT: The conformational dependence of the circular dichroism (CD) spectrum of a chiral molecule, α -hydroxyphenylacetic acid (HPAA) containing phenyl, COOH, OH and H groups around a chiral carbon atom, has been studied theoretically by using the SAC-CI (symmetry adapted cluster–configuration interaction) theory. The results showed that the CD spectrum of HPAA depends largely on the rotations (conformations) of the phenyl and COOH groups around the single bonds. The first band is due to the excitation of electrons belonging to the phenyl region and therefore sensitive to the phenyl rotation. The second band is due to the excitation of electrons belonging to the COOH region and therefore sensitive to the COOH rotation. From the comparison of the SAC-CI CD spectra calculated at various conformations of phenyl, COOH, and OH groups with the experimental spectrum, we could predict the stable geometry of this molecule, which agreed well with the most stable conformation deduced from the energy criterion. We also calculated the Boltzmann averaged spectrum and obtained better agreement with the experiment. Further, we performed preliminary investigations of the temperature dependence of the CD spectrum of HPAA. In general, the CD spectra of chiral molecules are very sensitive to low-energy processes like the rotations around the single bonds. Therefore, one should be able to study the natures of the weak interactions by comparing the SAC-CI spectra calculated at different geometries and conditions with the experimental spectrum using a new methodology we have termed ChiraSac.



1. INTRODUCTION

The molecular property of chirality is essential for biological specificity. Molecules with the same basic composition, but with centers of different chirality often show completely different biological activities.¹ Recently, we studied various samples of DNA² to clarify the relationships between their helical structures and their circular dichroism (CD) spectra. We used the symmetry adapted cluster–configuration interaction (SAC-CI) method,^{3–8} which is one of the most reliable excited-state theoretical methods. The SAC-CI method has been applied to the study of various aspects of molecular^{7–9} and biological^{10,11} spectroscopy. We have shown² that the observed CD spectrum of deoxyguanosine (dG), a component of the DNA we studied, strongly depended on its conformation, as defined by the dihedral angle between deoxyribose and guanine. The CD spectra of dG under different conditions were very sensitive to the conformational and structural changes near the chiral atoms in the molecule, even though these changes occurred with only small energy differences. The SAC-CI method describes the CD spectra of molecules very reliably,^{2,12–14} suggesting that the SAC-CI method can be a useful tool for elucidating the natures of low-energy motions and weak interactions that chiral molecules undergo. Such studies will contribute to our understanding of the weak interactions in solutions, and the chiral interactions in biological and medicinal systems.

Several recent reports demonstrated that the CD spectra of chiral molecules are sensitive to conformational changes of the molecules.^{15–27} If a molecule is conformationally flexible, it is difficult to estimate its most stable conformation only from the experimental CD spectrum. However, when we have theoretical information that links the CD spectrum to the conformation, the conformation of the molecule may be determined by comparing its experimental CD spectrum with the theoretical spectra calculated at its various conformations. Since poor reliability of the theoretical CD spectral data²⁸ would lead to ambiguities and difficulties, we need a highly reliable theory.

The SAC-CI method is included in the current version of the *Gaussian 09* suite of programs.²⁹ The Hartree–Fock (HF) method and density-functional theory (DFT)³⁰ provide reliable ground-state structures for chiral molecules at lower computational cost than the SAC-CI method. The polarizable continuum model (PCM)³¹ provides the solvent effects. The QM/MM method¹¹ provides detailed information about the molecular interactions due to the surrounding molecules and environments such as proteins and DNA. The AMBER³² and CHARMM³³ etc. methods provide force fields for biomolecules. Recently, the time-dependent density functional theory

Received: July 31, 2013

Revised: November 10, 2013

Published: November 20, 2013

(Td-DFT) calculations using the PBE0 functional give us reasonable agreement with the SAC-CI results.^{34,35} Although the SAC-CI method is more expensive than the Td-DFT method, the SAC-CI method provides more reliable prediction of spectroscopic properties. Many theoretical methods useful for such investigations are included in the current version of *Gaussian 09*.²⁹

Using this useful suite of programs, we have undertaken a “ChiraSac” project. “ChiraSac”, a term derived from chirality and SAC-CI, is a molecular technology that we are developing for studying the chemistry of chiral molecules and their interactions with the molecular environments by means of their CD and circularly polarized luminescence (CPL) spectra. An overview diagram of a “ChiraSac” project is shown in Figure 1.

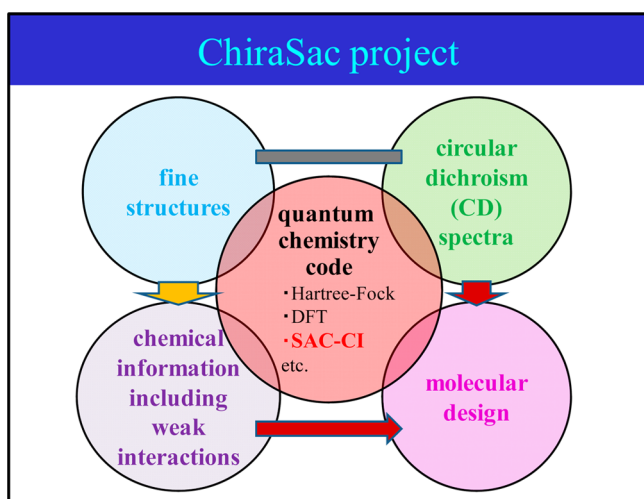


Figure 1. Overview diagram of ChiraSac project.

We use the SAC-CI methodology as a key reliable method of calculating the theoretical CD and CPL spectra of chiral systems in various conformational and environmental freedoms. We also connect many other useful theoretical methods included in *Gaussian 09* to study the optimal geometries and the natures of the interactions with the environments of the chiral molecules. The SAC-CI method clearly describes the reliable relationships between the structures and the CD spectra of chiral molecules.^{2,12–14} A ChiraSac study provides chemical information about the stable geometries of chiral molecules in different solutions or in confined environments such as in proteins and in nanomaterials, as well as revealing the underlying information about the natures of the weak interactions involved therein. A ChiraSac study uses information obtained both from experiments and from theoretical calculations.

In the present paper, we study the UV and CD spectra of α -hydroxyphenylacetic acid (HPAA) as an application of ChiraSac. HPAA is also known as mandelic acid and has been applied for the treatment of urinary tract infections.³⁶ HPAA is one of the simplest chiral molecules with a phenyl group. The circular dichroism (CD) spectra of many aromatic chromophores have been summarized in an earlier review by Smith,³⁷ whose research group defined the benzene sector rule³⁸ and the benzene chirality rule.³⁹ Recently, the sector rule has been studied theoretically by using the time-dependent density functional theory (Td-DFT).⁴⁰ In HPAA, phenyl (C_6H_5), hydroxyl (OH), and carboxyl (COOH) groups are

bound to the chiral carbon (marked with *) by single bonds (Figure 2). These groups can rotate easily with small energy

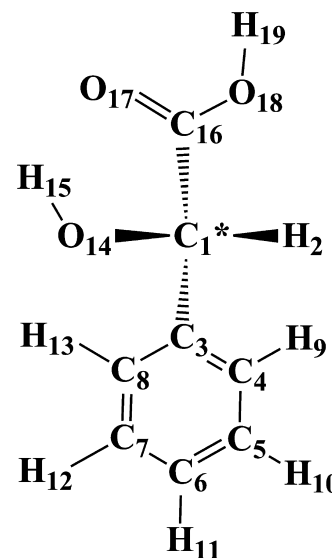


Figure 2. Atom labels of α -hydroxyphenylacetic acid.

barriers (see section 3.1). This is a general phenomenon since the chiral carbon is bound with four different single bonds. In this paper, we study the relations between the CD spectra and the rotation of the phenyl, hydroxyl, and carboxyl groups in HPAA. This study shows that a ChiraSac study can elucidate structural changes with low energy barriers in solution. Therefore, the ChiraSac study may provide structural information, which is necessary and important for molecular design.

2. COMPUTATIONAL CONDITIONS

The ground-state geometries of HPAA were optimized by DFT³⁰ using the B3LYP functional^{41,42} with the 6-31G(d) basis set. For the SAC/SAC-CI calculations, the D95(d)⁴³ basis set was employed, and the core orbitals of the C, O, and N atoms were treated as frozen orbitals, and all single and selected double excitation operators were included. Perturbation selections⁴⁴ were carried out with the threshold sets of 5×10^{-6} and 1×10^{-6} hartree for the SAC and SAC-CI calculations, respectively, and 10 excited states were calculated. The SAC-CI CD spectra were convoluted using Gaussian envelopes to describe the Franck–Condon widths and the resolution of the spectrometer. The full width at half-maximum (fwhm) of the Gaussian was taken to be 0.6 eV.

The rotatory strength (R_{0a}) of the CD spectra can be expressed by the length-gauge equation,⁴⁵ which is the imaginary part of the scalar product of the electric transition dipole moment (ETDM) and the magnetic transition dipole moments (MTDM) between the ground state (Ψ_0) and the excited state (Ψ_a),

$$R_{0a} = \text{Im}[\langle \Psi_0 | \hat{\mu} | \Psi_a \rangle \langle \Psi_a | \hat{m} | \Psi_0 \rangle] \quad (1)$$

where $\hat{\mu}$ is the electric dipole moment operator and \hat{m} is the magnetic dipole moment operator. However, since the ETDM of the eq 1 is gauge-origin dependent, we calculated the rotatory strength using the gauge-invariant velocity form given by the following equation.⁴⁶

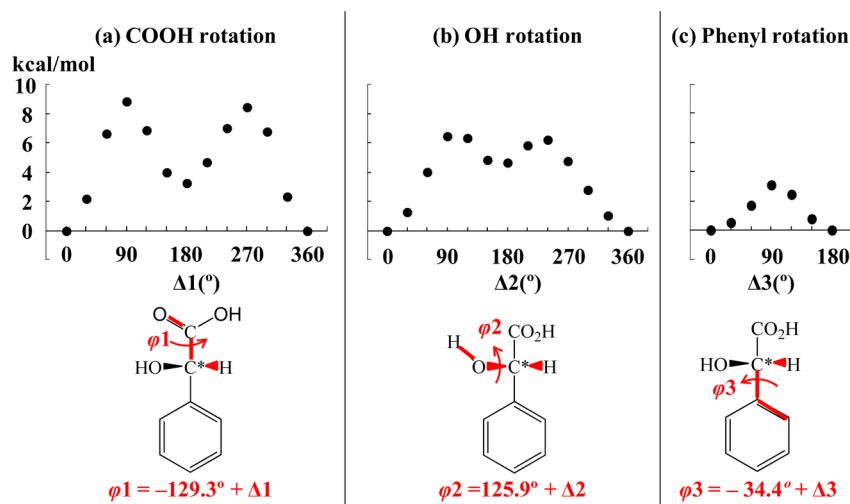


Figure 3. Potential energy curves for the (a) COOH, (b) OH, and (c) phenyl rotations of α -hydroxyphenylacetic acid, as a function of the dihedral angle change ($\Delta 1$, $\Delta 2$, $\Delta 3$) from the fully optimized dihedral angles $\phi_1 = -129.3$, $\phi_2 = 125.9$, and $\phi_3 = -34.4^\circ$.

$$R_{0a} = \text{Im} \left\{ \frac{\langle \Psi_0 | \nabla | \Psi_a \rangle \langle \Psi_a | \hat{m} | \Psi_0 \rangle}{E_a - E_0} \right\} \quad (2)$$

3. RESULTS AND DISCUSSION

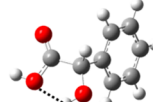
3.1. Ground-State Geometries. The fully optimized ground-state geometries of HPAAC with B3LYP/6-31G(d) (the most stable conformation) are shown in Supporting Information, (SI) Table S1. We calculated the potential energy curves using B3LYP/6-31G(d) for the ground state of HPAAC as a function of the dihedral angle changes ($\Delta 1$, $\Delta 2$, and $\Delta 3$) as shown in Figure 3. We used the dihedral angles $\text{O}_{17}=\text{C}_{16}-\text{C}_1^*-\text{H}_2$, $\text{H}_{15}-\text{O}_{14}-\text{C}_1^*-\text{H}_2$, and $\text{C}_4-\text{C}_3-\text{C}_1^*-\text{H}_2$ as shown in Figure 2 for the rotations of the carboxyl (COOH), hydroxyl (OH), or phenyl (C_6H_5) groups. The $\Delta = 0^\circ$ ($\Delta 1 = 0^\circ$, $\Delta 2 = 0^\circ$ or $\Delta 3 = 0^\circ$) corresponded to the most stable conformation of HPAAC obtained by the DFT method, B3LYP/6-31G(d). Notably, the geometries of the $\Delta 1 = 0^\circ$, $\Delta 2 = 0^\circ$ and $\Delta 3 = 0^\circ$ in Figure 3a–c were completely the same. For the phenyl rotation, $\Delta 3 = 180^\circ$ and $\Delta 3 = 0^\circ$ were essentially the same geometry. The fully optimized dihedral angles ϕ_1 , ϕ_2 , and ϕ_3 were calculated to be -129.3 , 125.9 , and -34.4° for the rotations of COOH, OH, and phenyl groups, respectively. Figure 4 shows the optimized geometries of HPAAC at several conformations. At the most stable conformation (Figure 4a), the hydrogen atom (H_{15}) of the OH group formed a hydrogen bond with the oxygen atom (O_{17}) of the $\text{O}=\text{C}$ group of COOH. This hydrogen bond accounted for this geometry being the most stable, and the two bulky phenyl and COOH groups were located at an appropriate distance. The dihedral angle (ϕ) was varied by the increment of 30° from $\Delta = 0^\circ$, and all of the geometrical parameters except for its dihedral angle were optimized.

The energy barriers were approximately 8.9, 6.5, and 3.1 kcal/mol for the COOH, OH, and phenyl rotations, respectively. The COOH and OH rotations broke their hydrogen bonding, so that the energy barriers for the rotations of COOH and OH were higher than that for the phenyl rotation. In the metastable conformation calculated at $\Delta 1 = 180^\circ$ for the COOH rotation, a hydrogen bond existed between the hydrogen atom (H_{15}) of the OH group and the oxygen atom (O_{18}) of the OH group of COOH as shown in Figure 4b.

(a) $\Delta = 0^\circ$ ($\Delta 1 = 0^\circ$, $\Delta 2 = 0^\circ$, $\Delta 3 = 0^\circ$)



(b) $\Delta 1 = 180^\circ$ (COOH rotation)



(c) $\Delta 2 = 180^\circ$ (OH rotation)

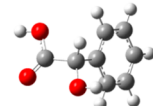


Figure 4. Optimized geometries of α -hydroxyphenylacetic acid at (a) $\Delta = 0^\circ$, the most stable conformation, (b) $\Delta 1 = 180^\circ$ of COOH rotation, which is 3.27 kcal/mol higher than $\Delta = 0^\circ$, and (c) $\Delta 2 = 180^\circ$ of OH rotation, which is 4.67 kcal/mol higher than $\Delta = 0^\circ$. The dotted lines represent the hydrogen bond.

Since the metastable conformation of the OH rotation cannot form a hydrogen bond with the $\text{O}=\text{C}$ group of the COOH group as shown in Figure 4c, the relative energy at $\Delta 2 = 180^\circ$ for the OH rotation was higher than that at $\Delta 1 = 180^\circ$ for the COOH rotation. However, the relative energies of the metastable conformations (approximately 3.2 and 4.6 kcal/mol for the rotations of COOH and OH, respectively) were higher than the rotational barrier of the phenyl group (approximately 3.1 kcal/mol). Then, at low temperature, the phenyl rotation seemed to play a more important role than the COOH and OH rotations. However, at high temperatures, all the rotations would become important.

3.2. Excited State of the Most Stable Conformation at $\Delta = 0^\circ$ ($\Delta 1 = 0^\circ$, $\Delta 2 = 0^\circ$ or $\Delta 3 = 0^\circ$). We compared in Table 1 the excitation energies, oscillator strengths, rotatory strengths, and the nature of the lowest six excited states for the most stable conformation at $\Delta = 0^\circ$ ($\Delta 1 = 0^\circ$, $\Delta 2 = 0^\circ$, or $\Delta 3 = 0^\circ$) with the experimentally observed values in water at 27°C .⁴⁷ The lowest excited state (1^1A) calculated at 4.66 eV (266 nm) was assigned to the lowest band at 4.77 eV (260 nm) of the experimental UV and CD spectra. This 1^1A excited state had

Table 1. Excited States of α -Hydroxyphenylacetic Acid at the Most Stable Conformation of $\Delta = 0^\circ$

	SAC-CI						exptl. ^a		
	(eV)	(nm)	Osc ^c	rot ^d		nature ^e	EE		
				(10^{-40} cgs)			(eV)	(nm)	
1 ¹ A	4.66	266	0.0007	-0.25		$\pi-\pi^*$	phenyl	4.77	260
2 ¹ A	5.45	227	0.03	+55.70		$n-\pi^*$	COOH	5.64	220
3 ¹ A	6.18	200	0.06	-22.23		$\pi-\pi^*$	phenyl		
4 ¹ A	6.95	178	0.53	-43.65		$\pi-\pi^*$	phenyl		
5 ¹ A	7.05	176	0.57	-8.10		$\pi-\pi^*$	phenyl		
6 ¹ A	7.16	173	0.15	0.41		$n-\pi^*$ (ET)	from OH to phenyl		

^aReference 47. ^bExcitation energy. ^cOscillator strength. ^dRotatory strength. ^eET represents electron transfer.

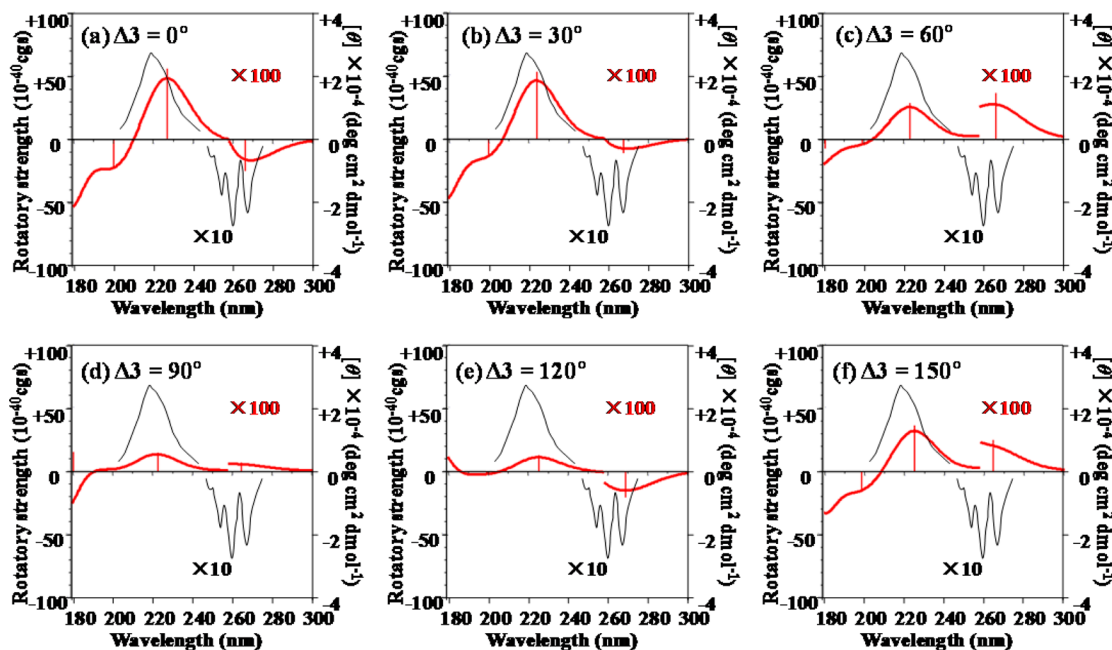


Figure 5. SAC-CI CD spectra (red lines) of α -hydroxyphenylacetic acid at several conformational angles of the phenyl rotation, compared with the experimental CD spectrum (black line).⁴⁷

very small oscillator and rotatory strengths and was characterized as the $\pi-\pi^*$ excitation of the phenyl group. This excited state corresponded to the forbidden transition of benzene with D_{6h} symmetry.

The 2¹A excited state calculated at 5.45 eV (227 nm) was assigned to the experimental band at 5.64 eV (220 nm). This excited state corresponded to the excitation of the nonbonding orbital to the π^* orbital of the COOH group. It has a weak oscillator strength but a strong rotatory strength.

Three excited states (3¹A, 4¹A, and 5¹A) were calculated at higher-energy regions in agreement with the experimental UV spectrum. These three excited states are characterized by strong oscillator and negative rotatory strengths and are composed of the $\pi-\pi^*$ excitations of the phenyl group.

In the 200–300 nm range, the experimental UV and CD spectra can be explained by the $\pi-\pi^*$ excitation of the phenyl group and the $n-\pi^*$ excitation of the COOH group. The SAC-CI UV spectrum was in good agreement with the experimental UV spectrum (see SI, Figure S1).

3.3. Conformational Dependence of the CD Spectra.

In Figures 5–7, we showed the SAC-CI CD spectra (red lines) of HPAAC calculated at several dihedral angles as compared with the experimental CD spectrum (black line).⁴⁷ The excitation energies, oscillator strengths, and rotatory strengths of 1 and

2¹A excited states appear in SI, Table S2. The dihedral angle (φ) was varied by the increment of 30° , while all other geometrical parameters were optimized at each angle. The experimental CD spectrum displays two bands above 200 nm. The lowest band was small and negative with vibrational modes at 260 nm. The second band was positive and strong at 220 nm. Figures 5, 6, and 7 show the variations of the CD spectra along with the rotations of the phenyl, carboxyl (COOH), and hydroxyl (OH) groups, respectively, from the most stable geometry $\Delta = 0^\circ$ ($\Delta_1 = 0^\circ$, $\Delta_2 = 0^\circ$ or $\Delta_3 = 0^\circ$). In all cases, we found that the experimental CD spectrum was in good accord with the SAC-CI CD spectrum calculated at the most stable conformation $\Delta = 0^\circ$ ($\Delta_1 = 0^\circ$, $\Delta_2 = 0^\circ$, or $\Delta_3 = 0^\circ$). From both calculated energy and CD spectra, $\Delta = 0^\circ$ should be the experimentally observed conformation.

For the phenyl rotation in Figure 5, the first CD band at 260 nm was negative for $\Delta_3 = 0, 30,$ and 120° but positive for $\Delta_3 = 60, 90,$ and 150° . The first band depended largely on the rotation of the phenyl group, because this band originates from the $\pi-\pi^*$ transition of this group (Table 1). On the other hand, the second band was positive for all conformations due to the $n-\pi^*$ transition of the COOH group (Table 1) and was not due directly to the $\pi-\pi^*$ transition of the phenyl group itself. However, the intensity was very small near the perpendicular

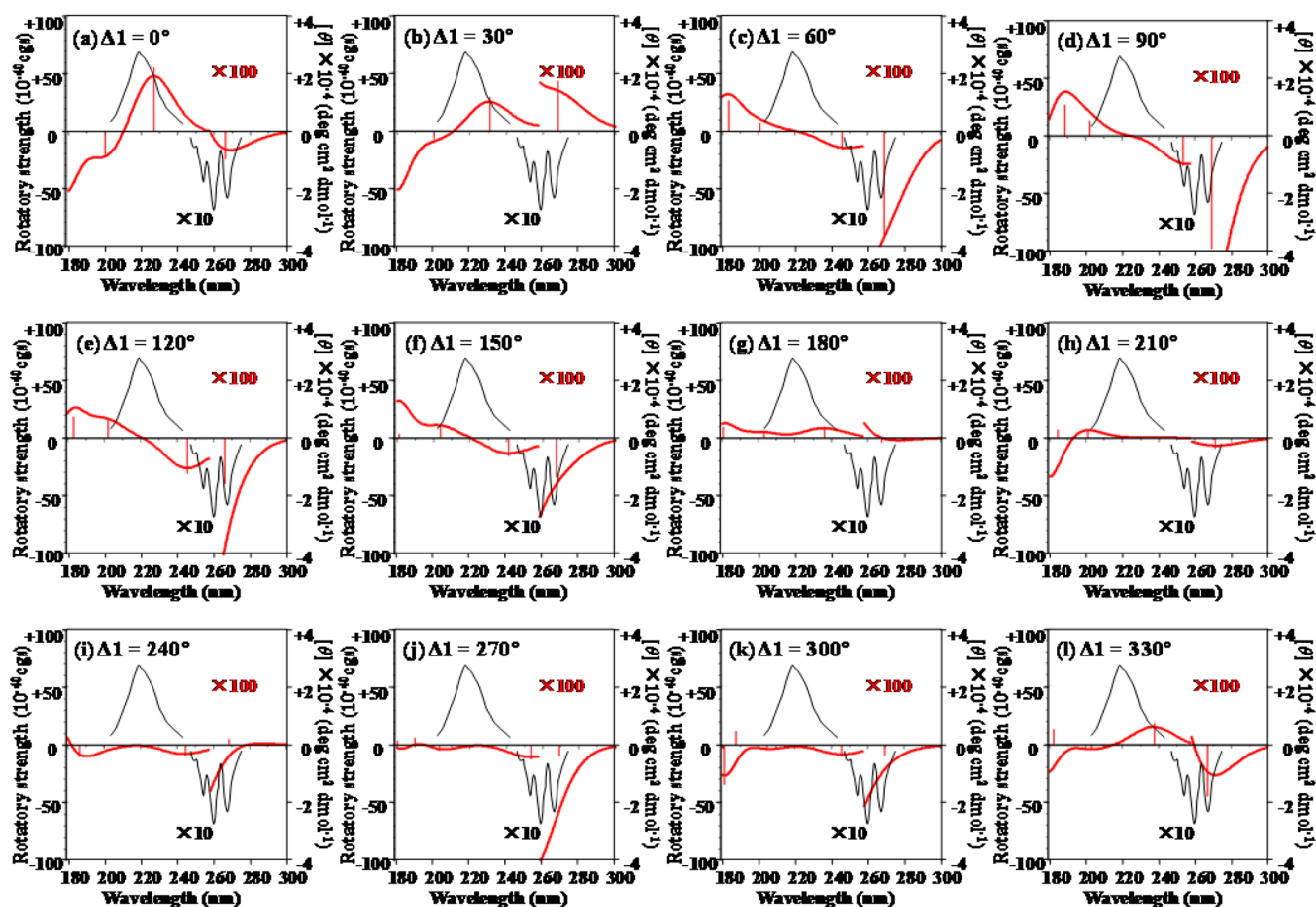


Figure 6. SAC-CI CD spectra (red lines) of α -hydroxyphenylacetic acid at several conformational angles of the carboxyl (COOH) rotation, compared with the experimental CD spectrum (black line).⁴⁷

orientation at $\Delta 3 = 90^\circ$. For the first band, the sign determined by the SAC-CI calculations agreed with the sign predicted by the sector rule except for the most unstable conformation ($\Delta 3 = 90^\circ$). Therefore, the sector rule is useful to predict the most stable conformation.

For the COOH rotation (Figure 6), the first CD band due to the π - π^* excitation of the phenyl group (Table 1) was fully negative except for $\Delta 1 = 30^\circ$, although the intensity depended on the extent of the COOH rotation. The dependence of the first CD band on the COOH rotation was smaller than that of the phenyl rotation (Figure 5). On the other hand, for the second band representing the n - π^* excitation of the COOH group (Table 1), the COOH rotation was drastically affected, as expected, not only by the sign and the intensity but also by the excitation energy itself. However, the energy barrier of the COOH rotation was higher than that for the phenyl rotation. Therefore, after the Boltzmann averaging, the effect of the COOH rotation was less significant than that of the phenyl rotation.

For the OH rotation given by Figure 7, the SAC-CI CD spectra were roughly similar among all conformations, because the excitations in the 200–300 nm range occur not in the OH group but in the phenyl and COOH regions (see Table 1). Therefore, the CD spectra were weakly dependent on the OH rotation.

The observed CD spectrum was most similar to the SAC-CI CD spectrum calculated at $\Delta = 0^\circ$ ($\Delta 1 = 0^\circ$, $\Delta 2 = 0^\circ$, or $\Delta 3 = 0^\circ$), which was also most favorable with respect to the energy

criterion. As shown in Figure 4a, the hydrogen bonding is an important factor of the stability of the $\Delta = 0^\circ$ conformation. However, this hydrogen-bonding interaction seems to have no effect on the CD spectra. Actually, for the OH rotation (Figure 7), the SAC-CI CD spectra at $\Delta 2 = +30^\circ$ and -30° (330°) do not change much from that at $\Delta = 0^\circ$ ($\Delta 2 = 0^\circ$), though the hydrogen-bonding interaction should be broken at $\Delta 2 = +30^\circ$ and -30° . The distance between O_{17} and H_{15} is 2.04 Å at $\Delta = 0^\circ$, 2.24 Å at $\Delta = +30^\circ$, and 2.18 Å at $\Delta = -30^\circ$ (330°). While this is an interesting observation, we must verify its general application with other examples. For the COOH rotation (Figure 6), the SAC-CI CD band at 220 nm changed drastically at $\Delta 1 = +30^\circ$ and -30° from that at $\Delta = 0^\circ$, because this band is due to the n - π^* transition of the COOH group itself. Both n and π^* MOs themselves change markedly by this rotation, as noted in section 3.5, so that we cannot attribute this change only to the breaking of the hydrogen bonding.

In more complex systems, it is often difficult to calculate reliable energies, because the modeling, assumptions, etc. must be introduced into the calculations of complex systems. Even in such cases, the reliability of the SAC-CI theory would make it possible to estimate the probable geometry of a chiral molecule only from the theoretical CD spectrum. For example, if the experimental CD spectrum of HPAA at some confined environment resembles the theoretical spectra shown in Figures 5–7, we can predict that its experimental geometry may be used in that calculation. When chemical interactions of the environment affect the CD spectrum of HPAA, we can perform

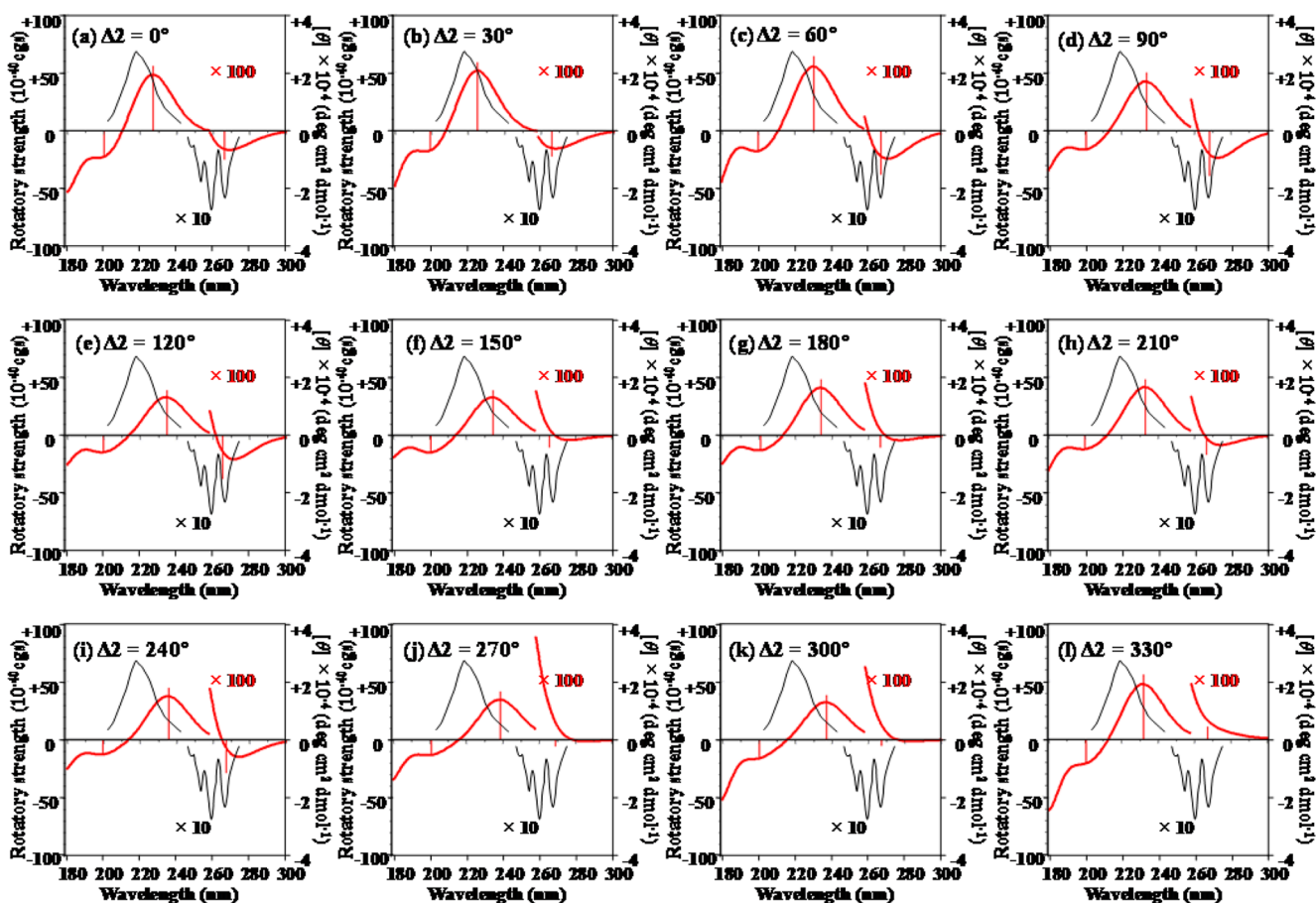


Figure 7. SAC-CI CD spectra (red lines) of α -hydroxyphenylacetic acid at several conformational angles of the hydroxyl (OH) rotation, compared with the experimental CD spectrum (black line).⁴⁷

some model calculations using a QM/MM method. In this case, we used a QM model that includes such chemical interactions.

3.4. Molecular Orbital Analysis of the Conformational Dependence of the CD Spectra on the Phenyl Rotation.

The origin of the change in the CD spectrum (Figure 5) caused by the phenyl rotation (Figure 3) may be analyzed from the viewpoint of the molecular orbitals (MO), as illustrated by the MOs of HPAA at two different rotational angles of the phenyl group, $\Delta 3 = 0^\circ$ and $\Delta 3 = 90^\circ$ (Figure 8).

Six MOs shown in Figure 8 are related to the 1^1A and 2^1A excited states that correspond to the first and second bands. The main configurations of the 1^1A excited state were the excitations from HOMO-1 to LUMO and from HOMO to LUMO+1. The 2^1A excited state corresponds to the excitation from the nonbonding (HOMO-3) orbital to the π^* (LUMO+2) orbital mainly localized at the C=O region of the COOH group. For each MO, two figures seen from the top and from the side were shown in Figure 8, where the side view is from the arrow shown in the top view.

The rotatory strength (R_{0a}) of the CD spectra, given by eq 1, is expressed using the angle θ between the electric transition dipole moment (ETDM) $\vec{\mu}_{0a}$ and the magnetic transition dipole moment (MTDM) \vec{m}_{0a} as

$$R_{0a} = \text{Im}[\vec{\mu}_{0a} \parallel \vec{m}_{0a} | \cos \theta] \quad (3)$$

The rotational strength is nonzero when the transition is optically active ($\vec{\mu}_{0a} \neq 0$), MTDM is nonzero ($\vec{m}_{0a} \neq 0$), and the angle $\theta \neq 90^\circ$. In molecules with high symmetry, the

rotatory strength is equal to zero, because the ETDM and MTDM are orthogonal, even when both ETDM and MTDM have some values. However, in chiral molecules, the above three conditions are always satisfied, except for the case where the two moments (ETDM and MTDM) are accidentally orthogonal to each other. We analyzed the MOs by changing the conformations to predict the rotatory strength without high-cost computations.

The HOMO-1, HOMO, LUMO and LUMO+1 were related to the 1^1A excited state and were mainly localized at the phenyl group (Figure 8). However, the LUMO at $\Delta 3 = 0^\circ$, in particular, spread out to the COOH group. Namely, the angle θ deviates from 90° . This is why the 1^1A excited state, which corresponds to the forbidden transition in benzene, changed to become optically active in HPAA. However, at $\Delta 3 = 90^\circ$, the LUMO became rather localized on the phenyl region, which accounts for the weaker intensity of the SAC-CI CD spectrum at $\Delta 3 = 90^\circ$ than at $\Delta 3 = 0^\circ$.

The HOMO-3 (nonbonding orbital) and LUMO+2 (π^* orbital) were related to the 2^1A excited state and were mainly localized at the COOH group. At $\Delta 3 = 0^\circ$, the orbitals of the COOH group interact with the π and π^* orbitals of phenyl group, but at $\Delta 3 = 90^\circ$, they interact with the σ and σ^* orbitals of the phenyl group. Since two MOs are not localized at the COOH group, the $n-\pi^*$ state also has some value in the CD spectra. These MOs at $\Delta 3 = 0^\circ$ are more greatly spread from the COOH group to the phenyl group than those at $\Delta 3 = 90^\circ$.

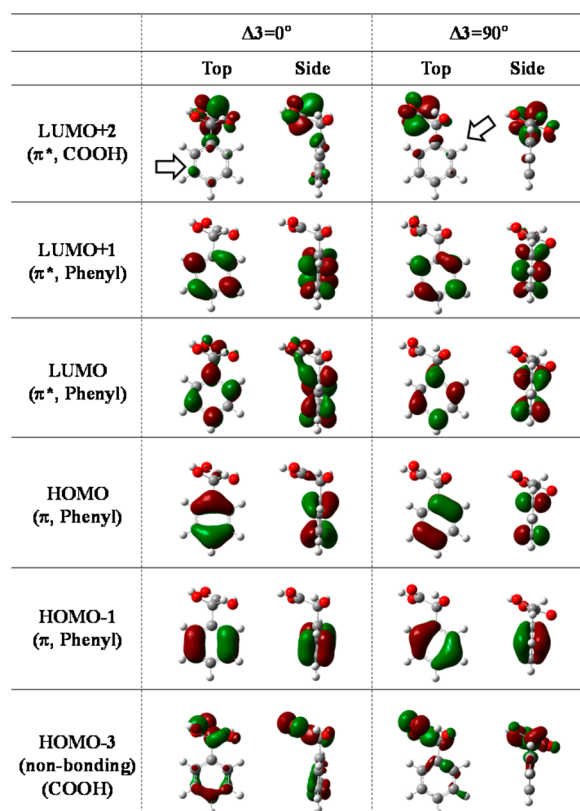


Figure 8. Molecular orbital pictures of the π and π^* orbitals of the phenyl group and the nonbonding and π^* orbitals of the COOH group at $\Delta 3 = 0$ and 90° in the phenyl rotation. "Side" is the figure seen from the arrow in "Top". The contour value of the isosurfaces is 0.05.

Therefore, the intensity of the 2^1A excited state becomes stronger at $\Delta 3 = 0^\circ$ than at $\Delta 3 = 90^\circ$.

These results indicate that the sign and the intensity of the CD spectra may be estimated by analyzing the nature of the excited states. Therefore, when a chiral molecule is put into a confined environment with only steric hindrance, we can predict its conformation by comparing the experimental CD spectrum with the SAC-CI spectrum of a free chiral molecule model. But, when the chiral molecules interact with the surrounding systems, the CD spectrum might be more affected by the surroundings rather than by the changes in the rotational angles. In such a case, the model calculation must include the chiral molecule as well as the surrounding molecular system by using, for example, the QM/MM method.

3.5. The Relationship between the 2^1A Excited State and the COOH Rotation. As shown in Figure 6, the COOH rotation largely affects the SAC-CI CD spectrum at ~ 220 nm, because the 2^1A excited state at ~ 220 nm is due to the $n-\pi^*$ excitation of the COOH group. Figure 9a shows the excitation energies of the 2^1A excited state at several conformational angles of the COOH rotation. This figure is very similar to the potential energy curve of the COOH rotation shown in Figure 3a. It is interesting to examine this correlation.

At the most stable conformation, HPA has a hydrogen bonding between the oxygen atom (O_{17}) of the $O=C$ group of COOH and the hydrogen atom (H_{15}) of the OH group (Figure 4a). However, when the angle ($\Delta 1$) changes from $\Delta 1 = 0^\circ$, the hydrogen bond becomes weaker. At $\Delta 1 = 180^\circ$, the oxygen atom (O_{18}) of the OH group of COOH seems to form a

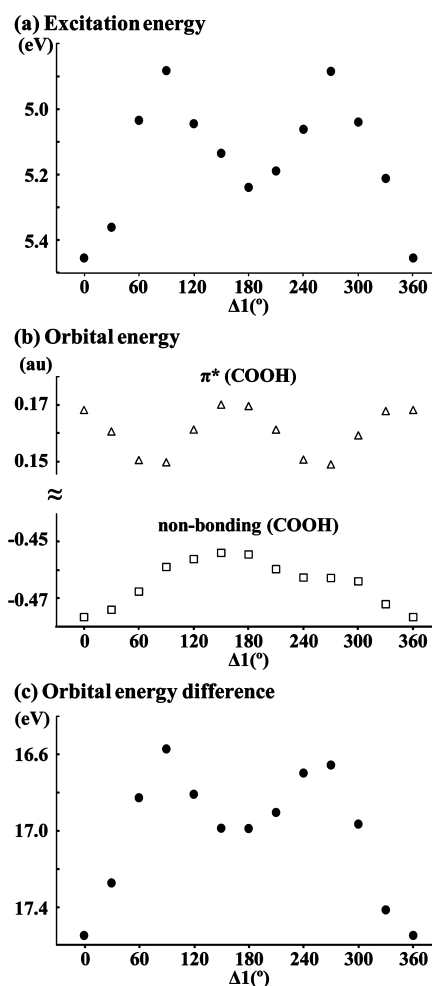


Figure 9. (a) Excitation energy of the 2^1A excited state, (b) orbital energies of the nonbonding and π^* orbitals, and (c) energy difference between the nonbonding and π^* orbitals, at several conformational angles of the carboxyl (COOH) rotation.

hydrogen bond to the hydrogen atom (H_{15}) of the OH group (Figure 4b). Since the oxygen atom (O_{18}) of the OH group of COOH is already linked to the hydrogen atom (H_{19}) by a covalent bond, the nonbonding orbital is unstable. Therefore, the nonbonding orbital of COOH is most stable at $\Delta 1 = 0^\circ$ (Figure 9b).

The π^* orbital of COOH is mainly localized on the COOH group but slightly delocalized onto the phenyl group. At $\Delta 1 = 90$ and 270° , this orbital is also spread to the OH group (see SI, Figure S2). However, this delocalization does not occur at $\Delta 1 = 0$ and 180° . Therefore, at $\Delta 1 = 90$ and 270° , the π^* orbital (COOH) becomes stabilized by the interaction with the OH group shown in Figure 9b. The change in the orbital energy difference between the nonbonding and π^* orbitals (COOH), as shown in Figure 9c, is similar to the change of the $n-\pi^*$ excitation energy (Figure 9a) or the ground-state potential curve (Figure 3a). As a result, the $n-\pi^*$ excitation energy is decreased in the unstable conformation (4.88 eV at $\Delta 1 = 90^\circ$ and 4.89 eV at $\Delta 1 = 270^\circ$) but higher in the stable conformation (5.45 eV at $\Delta 1 = 0^\circ$ and 5.23 eV at $\Delta 1 = 180^\circ$). Thus, the $n-\pi^*$ excitation energy is changed largely by the COOH rotation.

As noted in section 3.3, the shape of the CD spectrum is largely dependent on the COOH rotation (Figure 6). In

particular, at $\Delta 1 = 210^\circ$, since the rotatory strength is very weak for both 1^1A and 2^1A excited states, the SAC-CI CD spectrum is almost flat. The HOMO-1, HOMO, LUMO, LUMO+1 (π and π^* orbitals) are related to the 1^1A excited state and are localized at the phenyl group (similar to the MOs at $\Delta 3 = 90^\circ$ of the phenyl rotation in Figure 8). Therefore, for the 1^1A excited state, the intensity becomes very weak at $\Delta 1 = 210^\circ$, as the rotatory strength is always zero for symmetrical benzene. Next, we compared the MOs at $\Delta 1 = 210^\circ$ with those at $\Delta 1 = 0^\circ$ (Figure 10). At $\Delta 1 = 0^\circ$, the 2^1A excited state is mainly the

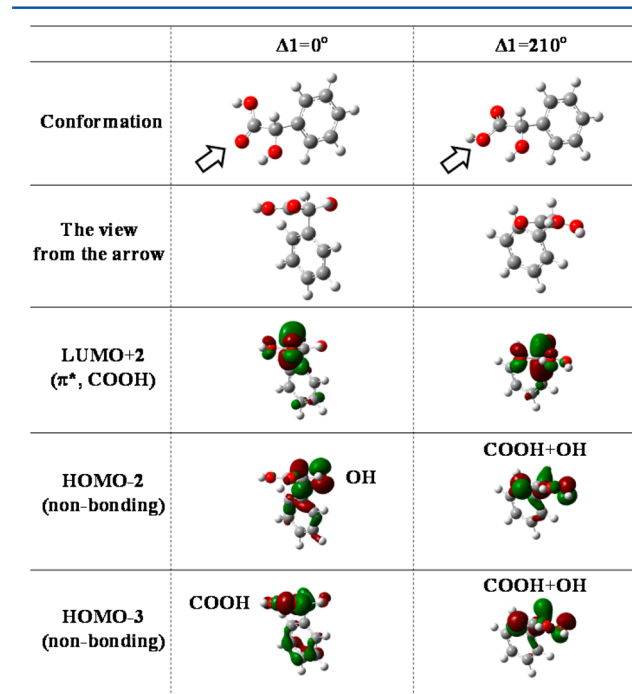


Figure 10. Molecular orbital pictures of the nonbonding orbitals of the COOH and OH groups and the π^* orbitals of the COOH group at $\Delta 1 = 0$ and 210° in the COOH rotation. MOs are the figure seen from the arrow in "Conformation". The contour value of the isosurfaces is 0.05.

excitation from the nonbonding orbital (HOMO-3) to the π^* orbital (LUMO+2). However, at $\Delta 1 = 210^\circ$, the two excitations from the nonbonding orbitals (HOMO-3 (COOH) and HOMO-2 (OH)) to the π^* orbital (LUMO+2) equally contribute to the 2^1A excited state. The coefficients of HOMO-3 and HOMO-2 to LUMO+2 are 0.55 and 0.60, respectively. Both HOMO-3 and HOMO-2 are almost symmetrical to the COOH-C*–OH plane to each other. Therefore, the rotatory strength is very weak by the cancellation of the two excitations. In summary, at $\Delta 1 = 210^\circ$, for both 1^1A and 2^1A excited states, the rotatory strength becomes very weak, and so the SAC-CI CD spectrum is flat.

The molecular orbitals of LUMO-3 to HOMO+2 at several dihedral angles are shown in SI, Figures S3–S5, and the angle θ is also shown in SI, Table S2.

3.6. Boltzmann Averaged Spectra. As seen from Figure 3, the energy barriers around the rotations are not large particularly for the phenyl rotation. Therefore, the observed spectrum may reflect the statistical averaging of the rotations. Therefore, we calculated the existence ratios of each conformer among 864 ($6 \times 12 \times 12$) conformers of HPAA, assuming the Boltzmann distribution. We performed the calculations at 27 °C (an experimental condition), 127, 227, 327, 427, and 527

°C, using the ground-state B3LYP/6-31G(d) energies. Table 2 shows the existence ratios of the conformers to be more than

Table 2. Top 14 highest existence ratios among the 864 conformers of α -hydroxyphenylacetic acid from the Boltzmann distributions at 27 °C and 527 °C

dihedral angle change (deg) ^a			existence ratio (%)		relative energy (kcal/mol)
phenyl ($\Delta 3$)	COOH ($\Delta 1$)	OH ($\Delta 2$)	27 °C	527 °C	
0	0	0	28.3	3.3	0.00
30	0	0	12.0	2.4	0.51
150	0	0	7.8	2.0	0.77
0	30	330	6.8	1.9	0.85
0	0	330	4.9	1.7	1.05
150	0	30	4.1	1.6	1.14
30	0	330	3.4	1.5	1.26
0	0	30	3.3	1.5	1.29
30	30	330	3.2	1.5	1.29
150	330	30	3.0	1.4	1.33
0	330	30	2.0	1.2	1.57
30	0	30	1.7	1.2	1.67
60	0	0	1.7	1.2	1.68
30	330	30	1.3	1.0	1.83
other 850 conformers			16.5	76.6	

^a $\Delta = 0^\circ$ at the most stable conformation.

1% at 27 and 527 °C. The top 14 stable conformers shown in Table 2 accounted for 83.5% at low temperature (27 °C) but for only 23.4% at high temperature (527 °C). Therefore, at high temperature, we need to consider all the conformers, not only the stable conformers.

Figure 11 shows the Boltzmann averaged SAC-CI CD spectrum at 27–527 °C. The spectrum obtained at 27 °C is

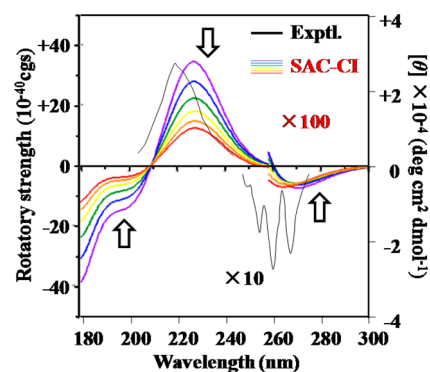


Figure 11. Boltzmann averaged SAC-CI CD spectra of α -hydroxyphenylacetic acid at 27 (purple line), 127 (blue line), 227 (green line), 327 (yellow line), 427 (orange line) and 527 °C (red line), compared with the experimental CD spectrum (27 °C, black line).⁴⁷ Arrows indicate the changes in raising the temperature.

similar to the SAC-CI CD spectrum of the most stable conformer. As the temperature increased, the intensity decreased in all bands. This observation is due to the fact that the contribution of the unstable conformers to the sign and intensity of the CD spectra increases as the temperature increases. The experimental confirmation of this theoretical prediction will be an interesting undertaking that awaits further study. The Boltzmann averaged SAC-CI CD spectra using the single-point CCSD/6-31G(d) energies at the B3LYP/6-

31G(d) geometries were similar to those using the ground-state B3LYP/6-31G(d) energies (see SI Table S3 and Figure S6).

4. CONCLUSION

We have studied the conformational dependence of the CD spectrum of α -hydroxyphenylacetic acid (HPAA) by using the SAC-CI method and compared it with the experimental spectrum as one of the examples derived from the “ChiraSac” project. The SAC-CI CD spectrum calculated at the most stable conformation of the phenyl, COOH, and OH rotations was in good agreement with the experimental CD spectrum. In other words, both calculated energy and CD spectra predicted that the geometry given by $\Delta = 0^\circ$ in Figure 4a should be the experimentally observed conformation. The potential energy barrier of the rotation was smallest for the phenyl group, and largest for the COOH, while that of OH rotation was intermediate. For the first $\pi-\pi^*$ excitation of the phenyl group at the 260 nm region (1^1A), the CD spectrum was strongly dependent on the phenyl rotation but weakly dependent on the COOH and OH rotations. For the second $n-\pi^*$ excitation of the COOH group at the 220 nm region (2^1A), the CD spectrum was strongly dependent on the COOH rotation but weakly dependent on the phenyl and OH rotations. Since the potential energy barrier of the phenyl rotation was smaller than that of the COOH and OH rotations, the effect of the phenyl rotation was more important than the COOH and OH rotations after Boltzmann averaging. The OH rotation was insensitive for both bands, because in the observed excitation energy region, the OH did not contribute to the excitations. Thus, the hydrogen bonding shown in Figure 4a must be an important factor for the stability of this geometry but has little effect on the CD spectra in the observed CD spectrum of HPAA. However, if the excitation of OH is observed in the CD spectra, the hydrogen -bonding must affect the shape and sign of the CD spectra. We omitted the solvent effect in this paper, but the study of the solvent effect is a very interesting subject.

The CD spectra of HPAA reflect the sensible changes of the molecular orbitals under the conformational changes. The HOMO-1, HOMO, and LUMO+1 were similar between two extreme conformations ($\Delta 3 = 0^\circ$ and $\Delta 3 = 90^\circ$ of the phenyl rotation), but the HOMO-3, LUMO, and LUMO+2 were clearly different as shown in Figure 8. Therefore, we could estimate the intensity of the CD spectra by examining the molecular orbitals responsible for the excitations. This outcome indicates that the molecular orbital analysis is useful for the understanding of the nature of the CD spectra.

The Boltzmann averaged SAC-CI CD spectrum as well as the SAC-CI CD spectrum of the most stable conformer were in good agreement with the experimental CD spectrum. As the temperature increased, the contribution of the unstable conformers to the CD spectrum increased. Therefore, it is necessary to take into account the Boltzmann averaging over the different conformers, when the energy barriers are small for the rotations. The temperature dependence of the CD spectrum of HPAA was predicted as shown in Figure 11. The experimental verification will be an interesting project in the future.

The SAC-CI method is useful for the study of the CD spectra, because of its high reliability. Our results indicate that the CD spectra are very sensitive to the conformational changes around the single bonds, which are generally low-energy processes. This means that, when the experimental CD

spectrum is compared with the reliable theoretical spectra calculated at several conformations, we can predict the stable conformation only from the CD spectroscopy. We expect that the CD spectroscopy would be a useful tool to investigate the nature of the weak interactions and the low-energy processes involved, similar to the usefulness of X-ray spectroscopy for crystals. Note that this is possible only when we have a very reliable theoretical method of calculating the CD spectra of molecules. The SAC-CI method has been proved to be just such a method. Our intention is to apply our “ChiraSac” methodology to many different phenomena of chiral molecules. This new technique should be especially useful for drug molecules.

■ ASSOCIATED CONTENT

Supporting Information

Coordinates (Table S1) and SAC-CI UV spectrum (Figure S1) of the most stable conformation, the 1 and 2^1A excited states (Table S2) and molecular orbital pictures (Figure S2–S5) for COOH, OH, or phenyl rotations, the ratio of conformers (Table S3), and Boltzmann averaged SAC-CI CD spectra (Figure S6) using CCSD/6-31G(d) energies. This material is available free of charge via the Internet at <http://pubs.acs.org>.

■ AUTHOR INFORMATION

Corresponding Authors

*E-mail: [t.miyahara\[at\]qcrci.or.jp](mailto:t.miyahara[at]qcrci.or.jp). Tel: +81-75-634-3211. Fax: +81-75-634-3211.

*E-mail: [h.nakatsuji\[at\]qcrci.or.jp](mailto:h.nakatsuji[at]qcrci.or.jp).

Notes

The authors declare no competing financial interest.

■ ACKNOWLEDGMENTS

The computations were performed using the computers at the Research Center for Computational Science, Okazaki, Japan, whom we acknowledge. We also thank the support of Mr. Nobuo Kawakami for the researches of QCRI.

■ REFERENCES

- (1) *Circular Dichroism: Principles and Applications*; Berova, N., Nakanishi, K., Woody, R. W., Eds; Wiley-VCH: New York, 2000.
- (2) Miyahara, T.; Nakatsuji, H.; Sugiyama, H. Helical Structure and Circular Dichroism Spectra of DNA: A Theoretical Study. *J. Phys. Chem. A* **2013**, *117*, 42–55.
- (3) Nakatsuji, H.; Hirao, K. Cluster Expansion of the Wavefunction. Symmetry-Adapted-Cluster Expansion, Its Variational Determination, and Extension of Open-Shell Orbital Theory. *J. Chem. Phys.* **1978**, *68*, 2053–2065.
- (4) Nakatsuji, H. Cluster Expansion of the Wavefunction. Excited States. *Chem. Phys. Lett.* **1978**, *59*, 362–364.
- (5) Nakatsuji, H. Cluster Expansion of the Wavefunction. Electron Correlations in Ground and Excited States by SAC (Symmetry-Adapted-Cluster) and SAC-CI Theories. *Chem. Phys. Lett.* **1979**, *67*, 329–333.
- (6) Nakatsuji, H. Cluster Expansion of the Wavefunction. Calculation of Electron Correlations in Ground and Excited States by SAC and SAC-CI Theories. *Chem. Phys. Lett.* **1979**, *67*, 334–342.
- (7) Nakatsuji, H. Electronic Structures of Ground, Excited, Ionized, and Anion States Studied by the SAC/SAC-CI Theory. *Acta Chim. Hung. Models Chem.* **1992**, *129*, 719–776.
- (8) Nakatsuji, H. SAC-CI Method: Theoretical Aspects and Some Recent Topics. In *Computational Chemistry Reviews of Current Trends*; Leszczynski, J., Ed; World Scientific: Singapore, 1997; Vol. 2, pp 62–124.

- (9) Ehara, M.; Ishida, M.; Toyota, K.; Nakatsuji, H. SAC-CI General-R Method: Theory and Applications to the Multi-Electron Processes. In *Reviews in Modern Quantum Chemistry (A tribute to Professor Robert G. Parr)*; Sen, K. D., Ed; World Scientific: Singapore, 2003; pp 293–319.
- (10) Hasegawa, J.; Ohkawa, K.; Nakatsuji, H. Excited States of the Photosynthetic Reaction Center of *Rhodospseudomonas Viridis*: SAC-CI Study. *J. Phys. Chem. B* **1998**, *102*, 10410–10419.
- (11) Fujimoto, K.; Hasegawa, J.; Nakatsuji, H. Color Tuning Mechanism of Human Red, Green, and Blue Cone Pigments: SAC-CI Theoretical Study. *Bull. Chem. Soc. Jpn.* **2009**, *82*, 1140–1148.
- (12) Honda, Y.; Kurihara, A.; Hada, M.; Nakatsuji, H. Excitation and Circular Dichroism Spectra of (–)-(3a*S*,7a*S*)-2-chalcogeno-trans-hydrindans (Ch = S, Se, Te): SAC and SAC-CI Calculations. *J. Comput. Chem.* **2008**, *29*, 612–621.
- (13) Miyahara, T.; Hasegawa, J.; Nakatsuji, H. Circular Dichroism and Absorption Spectroscopy for Three-Membered Ring Compounds Using Symmetry-Adapted Cluster-Configuration Interaction (SAC-CI) Method. *Bull. Chem. Soc. Jpn.* **2009**, *82*, 1215–1226.
- (14) Honda, Y.; Kurihara, A.; Kenmochi, Y.; Hada, M. Excitation and Circular Dichroism Spectra of (+)-(S,S)-bis(2-methylbutyl)-chalcogenides. *Molecules* **2010**, *15*, 2357–2373.
- (15) Niederalt, C.; Grimme, S.; Peyerimhoff, S. D.; Sobanski, A.; Vogtle, F.; Lutz, M.; Spek, A. L.; van Eis, M. J.; de Wolf, W. H.; Bickelhaupt, F. Chiroptical Properties of 12,15-Dichloro[3.0]-Orthometacyclophane—correlations between Molecular Structure and Circular Dichroism Spectra of a Biphenylophane. *Tetrahedron: Asymmetry* **1999**, *10*, 2153–2164.
- (16) Vogtle, F.; Grimme, S.; Hormes, J.; Dotz, K. H.; Krause, N. Theoretical Simulations of Electronic Circular Dichroism Spectra. In *Interactions in Molecules Electronic and Steric Effects*; Peyerimhoff, S. D., Ed; Wiley-VCH: Weinheim, 2003; pp 66–109.
- (17) Jorge, F. E.; Autschbach, J.; Ziegler, T. On the Origin of Optical Activity in Tris-diamine Complexes of Co(III) and Rh(III): A Simple Model Based on Time-Dependent Density Function Theory. *J. Am. Chem. Soc.* **2005**, *127*, 975–985.
- (18) Komori, H.; Inai, Y. Electronic CD Study of a Helical Peptide Incorporating Z-Dehydrophenylalanine Residues: Conformation Dependence of the Simulated CD Spectra. *J. Phys. Chem. A* **2006**, *110*, 9099–9107.
- (19) Crawford, T. D.; Tam, M. C.; Abrams, M. L. The Current State of Ab Initio Calculations of Optical Rotation and Electronic Circular Dichroism Spectra. *J. Phys. Chem. A* **2007**, *48*, 12057–12068.
- (20) Botek, E. Champagne, B. Circular dichroism of helical structures using semiempirical methods. *J. Chem. Phys.* **2007**, *127*, 204101-1–1204101-9.
- (21) Giorgio, E.; Tanaka, K.; Verotta, L.; Nakanishi, K.; Berova, N.; Rosini, C. Determination of the Absolute Configurations of Flexible Molecules: Synthesis and Theoretical Simulation of Electronic Circular Dichroism/Optical Rotation of Some Pyrrolo[2,3-*b*]indoline alkaloids—A case study. *Chirality* **2007**, *19*, 434–445.
- (22) Ding, Y.; Li, X. C.; Ferreira, D. Theoretical Calculation of Electronic Circular Dichroism of the Rotationally Restricted 3,8"-Biflavonoid Morelloflavone. *J. Org. Chem.* **2007**, *72*, 9010–9017.
- (23) Bringmann, G.; Gulder, T. A. M.; Reichert, M.; Gulder, T. The Online Assignment of the Absolute Configuration of Natural Products: HPLC-CD in Combination with Quantum Chemical CD Calculations. *Chirality* **2008**, *20*, 628–642.
- (24) Grkovic, T.; Ding, Y.; Li, X. C.; Webb, V. L.; Ferreira, D.; Copp, B. R. Enantiomeric Discorhabdin Alkaloids and Establishment of Their Absolute Configurations Using Theoretical Calculations of Electronic Circular Dichroism Spectra. *J. Org. Chem.* **2008**, *73*, 9133–9136.
- (25) Shimizu, A.; Mori, T.; Inoue, Y.; Yamada, S. Combined Experimental and Quantum Chemical Investigation of Chiroptical Properties of Nicotinamide Derivatives with and without Intramolecular Cation- π Interactions. *J. Phys. Chem. A* **2009**, *113*, 8754–8764.
- (26) Fan, J.; Ziegler, T. A Theoretical Study on the Exciton Circular Dichroism of Propeller-Like Metal Complexes of Bipyridine and Tripodal Tris(2-pyridylmethyl)amine Derivatives. *Chirality* **2011**, *23*, 155–166.
- (27) Lambert, J.; Compton, R. N.; Crawford, T. D. The Optical Activity of Carvone: A Theoretical and Experimental Investigation. *J. Chem. Phys.* **2012**, *136*, 114512-1–114512-12.
- (28) Leang, S. S.; Zahariev, F.; Gordon, M. S. Benchmarking the performance of time-dependent density functional methods. *J. Chem. Phys.* **2012**, *136*, 104101-1–104101-12.
- (29) Frisch, M. J.; Trucks, G. W.; Schlegel, H. B.; Scuseria, G. E.; Robb, M. A.; Cheeseman, J. R.; Scalmani, G.; Barone, V.; Mennucci, B.; Petersson, G. A.; et al. *Gaussian 09*; revision B.01; Gaussian Inc.: Wallingford, CT, 2010.
- (30) Parr, R. G.; Yang, W.; *Density-Functional Theory of Atoms and Molecules*; Oxford University Press: Oxford, 1989.
- (31) Tomasi, J.; Mennucci, B.; Cammi, R. Quantum mechanical continuum solvation models. *Chem. Rev.* **2005**, *105*, 2999–3093.
- (32) Cornell, W. D.; Cieplak, P.; Bayly, C. I.; Gould, I. R.; Merz, K. M., Jr.; Ferguson, D. M.; Spellmeyer, D. C.; Fox, T.; Caldwell, J. W.; Kollman, P. A. A Second Generation Force-Field for the Simulation of Proteins, Nucleic Acids, and Organic Molecules. *J. Am. Chem. Soc.* **1995**, *117*, 5179–5197.
- (33) Brooks, B. R.; Brucoleri, R. E.; Olafson, B. D.; States, D. J.; Swaminathan, S.; Karplus, M. CHARMM: A program for Macromolecular Energy, Minimization, and Dynamics Calculations. *J. Comput. Chem.* **1983**, *4*, 187–217.
- (34) Bousquet, D.; Fukuda, R.; Maitarad, P.; Jacquemin, D.; Ciofini, I.; Adamo, C.; Ehara, M. Excited-State Geometries of Heteroaromatic Compounds: A Comparative TD-DFT and SAC-CI Study. *J. Chem. Theory Comput.* **2013**, *9*, 2368–2379.
- (35) Ehara, M.; Fukuda, R.; Adamo, C.; Ciofini, I. Chemically Intuitive Indices for Charge-Transfer Excitation Based on SAC-CI and TD-DFT Calculations. *J. Comput. Chem.* **2013**, *34*, 2498–2501.
- (36) Putten, P. L. Mandelic Acid and Urinary Tract Infections. *Antonie van Leeuwenhoek* **1979**, *45*, 622–623.
- (37) Smith, H. E. Chiroptical Properties of the Benzene Chromophore. A Method for the Determination of the Absolute Configurations of Benzene Compounds by Application of the Benzene Sector and Benzene Chirality Rules. *Chem. Rev.* **1998**, *98*, 1709–1740.
- (38) Smith, H. E.; Fontana, L. P. Optically-Active Amines. 35. A Sector Rule for the Circular-Dichroism of the Benzene Chromophore. *J. Org. Chem.* **1991**, *56*, 432–435.
- (39) Pickard, S. T.; Smith, H. E. Optically-Active Amines. 34. Application of the Benzene Chirality Rule to Ring-Substituted Phenylcarbinamines and Carbinols. *J. Am. Chem. Soc.* **1990**, *112*, 5741–5747.
- (40) Pescitelli, G.; Di Bari, L.; Caporusso, A. M.; Salvadori, P. The Prediction of the Circular Dichroism of the Benzene Chromophore: TDDFT Calculations and Sector Rules. *Chirality* **2008**, *20*, 393–399.
- (41) Becke, A. D. Density-Functional Thermochemistry. III. The Role of Exact Exchange. *J. Chem. Phys.* **1993**, *98*, 5648–5652.
- (42) Lee, C.; Yang, W.; Parr, R. G. Development of the Colle-Salvetti Correlation-Energy Formula into a Functional of the Electron Density. *Phys. Rev. B* **1988**, *37*, 785–789.
- (43) Dunning, T. H., Jr.; Hay, P. J. In *Modern Theoretical Chemistry*; Schaefer, H. F. III, Ed.; Plenum: New York, 1976; Vol. 3, pp 1–28.
- (44) Nakatsuji, H. Cluster Expansion of the Wavefunction. Valence and Rydberg Excitations, Ionizations, and Inner-Valence Ionizations of CO₂ and N₂O Studied by the SAC and SAC-CI Theories. *Chem. Phys.* **1983**, *75*, 425–441.
- (45) Rosenfeld, L. Quantum Mechanical Theory of Natural Optical Activity of Liquids and Gases. *Z. Phys.* **1929**, *52*, 161–174.
- (46) Moffitt, W. Optical Rotatory Dispersion of Helical Polymers. *J. Chem. Phys.* **1956**, *25*, 467–478.
- (47) Verbit, L.; Heffron, P. J. Optically Active Aromatic Chromophores-IV. Circular Dichroism Studies of Some Open-Chain Systems. *Tetrahedron* **1968**, *24*, 1231–1236.